TURKEY

Circulation and Hydrography of the Levantine Basin (POEM–I–85 and POEM–II–86)

E. Özsoy, A. Hecht and Ü. Ünlüata

I. Introduction

Two major experiments during October-November 1985 (POEM–I–85) and March-April 1986 (POEM–II–86) respectively were completed in the Levantine Basin by the R/V BILIM of the IMS-METU and the R/V SHIKMONA of the ILOR within the context of the POEM program.

The hydrographic data were obtained at stations with a nominal spacing of 0.5° latitude and longitude (except in the northern half of the basin in March-April 1986 where the R/V BILIM experimented with 0.75° zonal and 0.5° meridional station spacing), covering the stations shown in Figs. 1a and 1b.

The combined data were analysed jointly, following an intercalibration of the temperature and salinity values.

II. Circulation

The density field obtained from the experiments was used to calculate the geopotential anomaly (dynamic depth anomaly) referenced to 800 db at every station, and the resulting values at each pressure level were objectively analyzed to yield the streamfunction fields, some of which are displayed in Figs. 2a, 2b, 3a and 3b.

We refer to the geopotential maps of October-November 1985 and March-April 1986 as the summer and winter circulations, because they characterize the main features of the two major seasons as well as the periods of maximum and minimum heat storage, respectively, within the basin.

The summer surface circulation map (Fig. 2a) reveals two major anticyclonic gyres in the southern part of the basin, which we refer to as the Mersa Matruh and the Shikmona gyres, and a cyclonic gyre centered at the Rhodes Basin, which is referred to as the Rhodes gyre. Between the Rhodes and the Mersa Matruh gyres, an intense jet flow with velocities of the order of 40 cm/sec^{-1}, which we refer to as the Central Levantine Basin Jet, proceeds towards Cyprus. There the current bifurcates and one of its branches flow northward and encircle the Rhodes gyre, while the other part flows east, later to become partly incorporated in the Shikmona anticyclonic circulation.

Smaller eddies appear within the major gyres as well as between them. At deeper levels (Fig. 2b), the anticyclonic eddies, i.e. the Mersa Matruh gyre, the Antalya and the southeastern Cyprus eddies, intensify and some of the anticyclonic gyres split into multiple centers. The eddy centers are shifted horizontally with depth. The cyclonic circulation seems to disintegrate with depth.

In the winter cruise, the surface circulation (Fig. 3a) reveals smaller scale features as compared to summer. The major gyres that were also observed in summer appear to be persistent although they display major deformations. The Rhodes gyre, which is now crescentic in shape, encircles the Mersa Matruh gyre with its southerly extensions. The Shikmona gyre can still be identified, although it has detached from the eastern end of the Mersa Matruh gyre. At depth, two major anticyclonic eddies survive.

III. Hydrography

The hydrography of the basin is extremely complex, with surface water (SW) in the summer overlying the Atlantic water (AW) entering the basin from the west, and the Levantine Intermediate Water (LIW) which is locally formed in winter. However, both the AW and the LIW appear in summer and winter in comparable quantities and become advected, entrained and entrapped by the eddies, leading to patchy distributions of both water types.

It is therefore necessary to relate the distribution of water masses to the circulation. Mesoscale stirring by eddies and isopycnal displacement processes often mask the processes leading to localized formation of LIW, and seem to be as important as the latter.

Within the Rhodes gyre, water properties are nearly homogenized by divergence and upwelling at the center. At the periphery, the LIW is trapped within anticyclonic eddies, or between those eddies and the coast. The AW is shown to be pooled within the Mersa Matruh gyre, overlying a deeper LIW salinity maximum. It is also evident that the AW is advected by the Central Levantine Basin Jet to be carried further between the gyres as narrow filaments.

Typical salinity sections from the summer and winter cruises are shown in Figs. 4 and 5, where the LIW can typically be identified with contours of $S > 38.95$ and AW can be identified with salinity values of $S < 38.90$.

To quantify the AW and LIW distributions, the vertical profiles of salinity were integrated between logically selected limits, i.e. $S < 39.1$ and $S < 39.0$ for AW in the summer and winter respectively, and $S > 38.9$ for LIW in both cruises. These limits were determined by examining the distribution of the maximum value of the minimum salinity for AW and the minimum of the maximum intermediate depth salinity for LIW at all stations. The differences of salinity from these limits were then integrated vertically, observing certain logical checks, to yield the positive and negative salt anomalies in units of kg m^{-2}, as a measure of LIW and AW anomalies. The salt anomaly maps are presented in Figs. 6a, 6b, 7a and 7b to emphasize the advection, trapping and stirring by eddies.

IV. Conclusions

The main features of the circulation reveal greater details as compared to previous descriptions in terms of the multiple scales of motion, vertical structure, interacting eddies, fronts and jets. The main difference from the earlier estimates emerges in the southern part of the basin, where clockwise currents along the coast are indicated, and also in the extent and area covered by the cyclonic circulation.

The numerous gyres and eddies appear to interact with the basin boundaries and topography as well as with each other, as being confined within the relatively small dimensions of the basin. During these processes of interaction, they advect as well as entrain the different water masses, leading to basin-scale stirring, concurrent with the water mass formation processes.

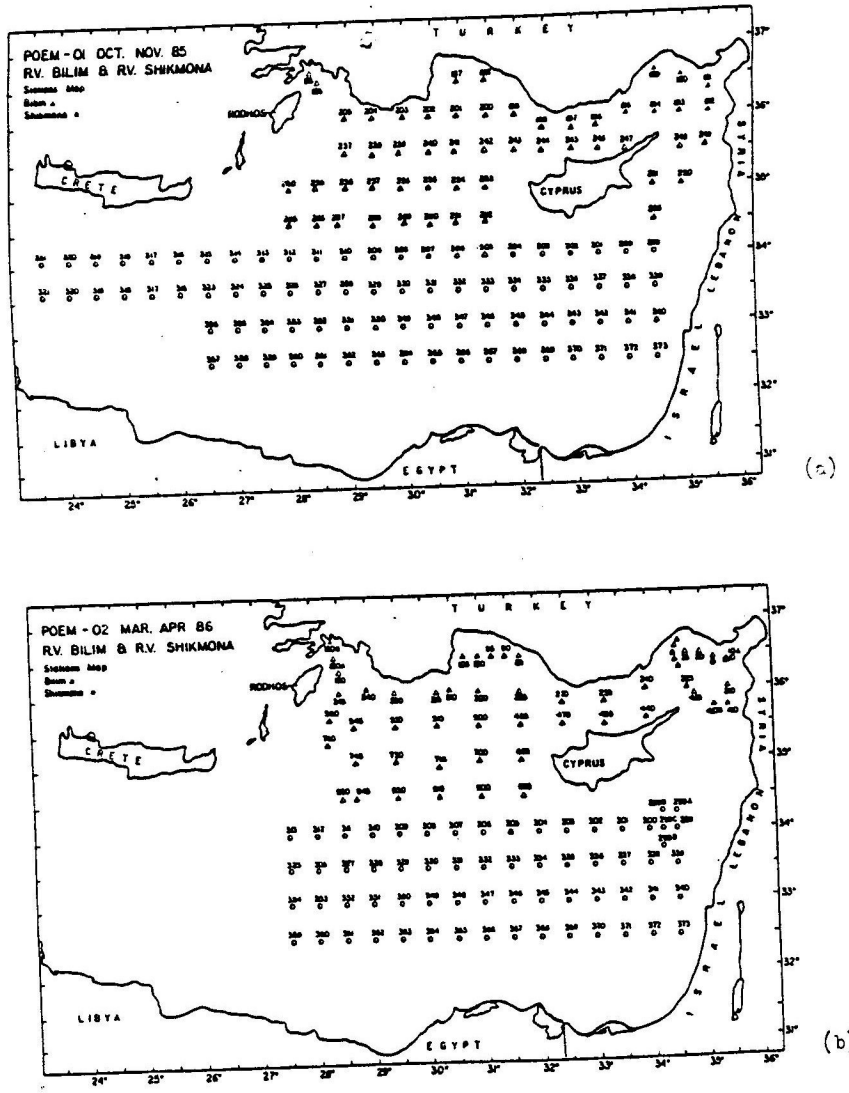

Fig. 1 Stations occupied by the R/V BILIM and R/V SHIKMONA (a) October-November 1985 and (b) March-April 1986.

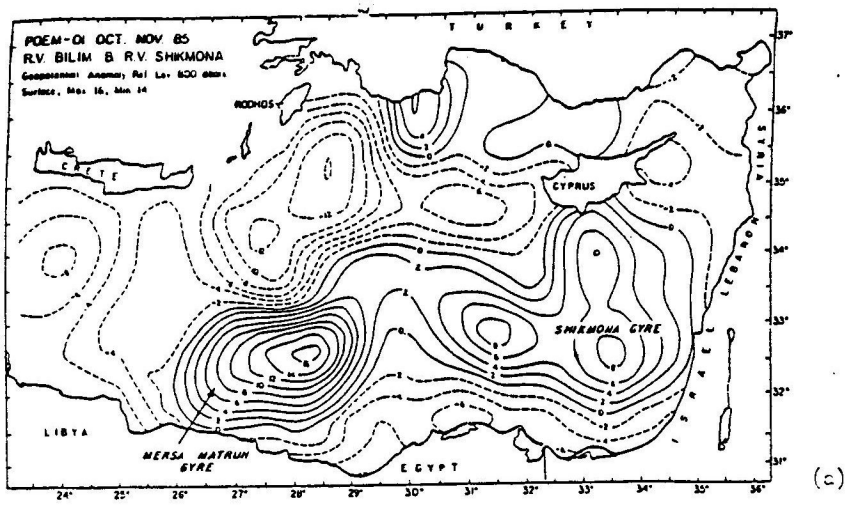

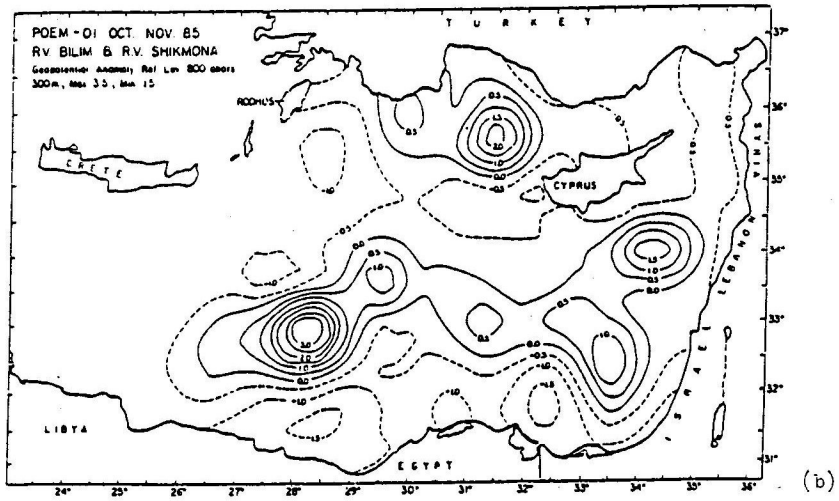

Fig. 2 Geopotential anomaly (in dynamic cm) referred to 800 db, October-November 1985 at (a) surface and (b) 300 db.

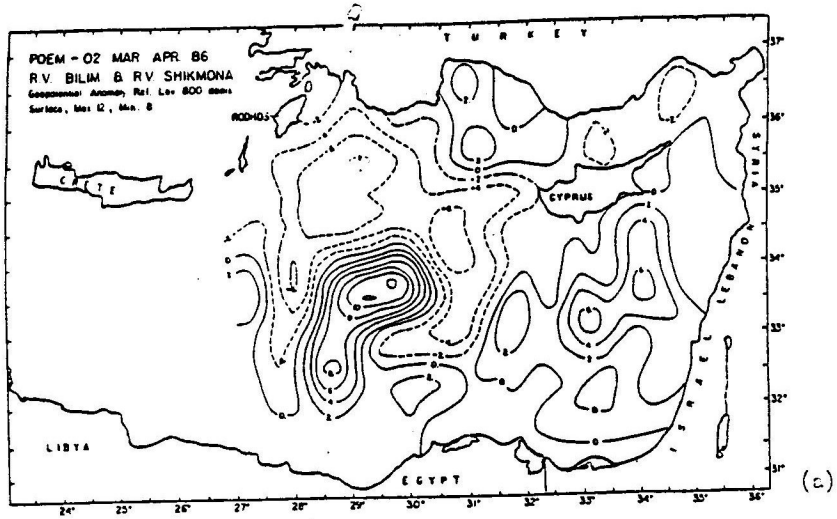

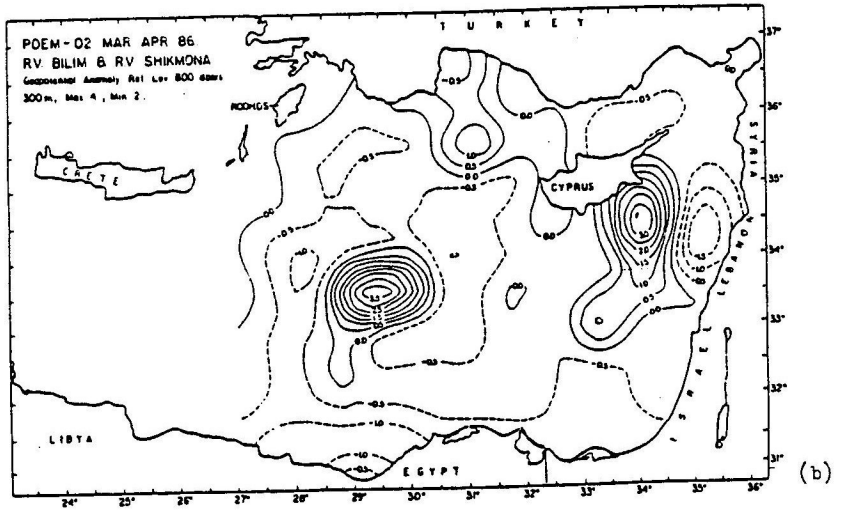

Fig. 3 Geopotential anomaly (in dynamic cm) referred to 800 db, March-April 1986 at (a) surface and (b) 300 db.

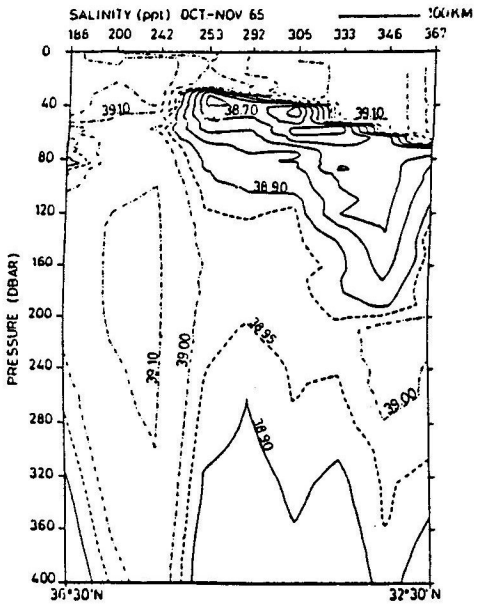

Fig. 4 North-South section of salinity, west of Cyprus, October-November 1985.

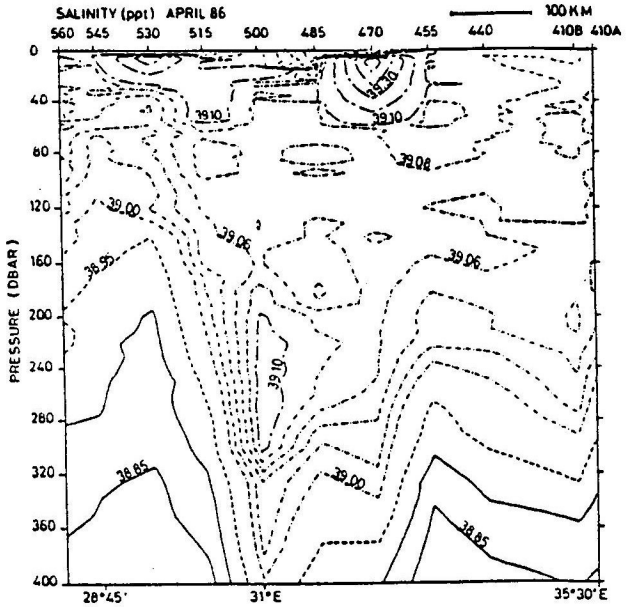

Fig. 5 East-West section of salinity, north of Cyprus, March-April 1986.

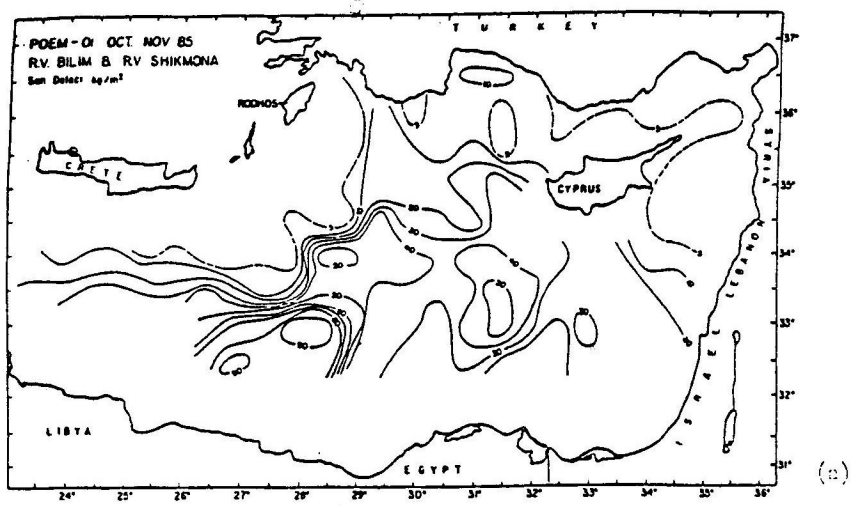

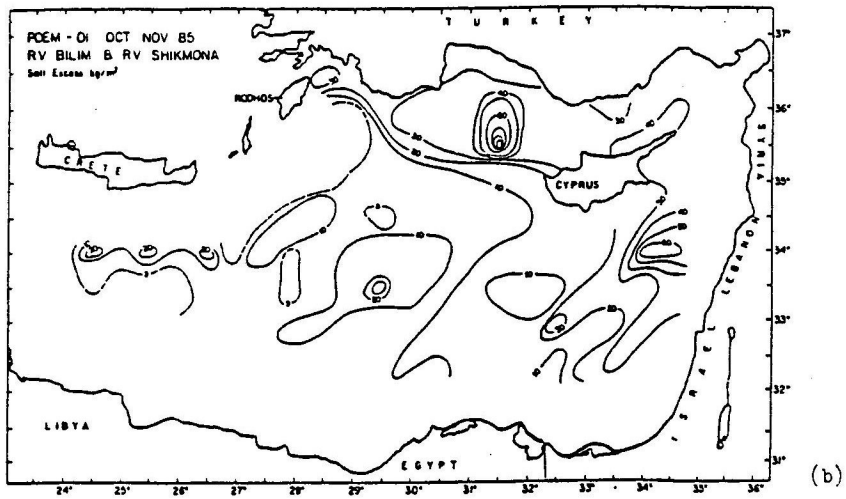

Fig. 6 Salt anomaly in units of kg m^{-2} integrated over the depth, October-November 1985. (a) Salt defect due to AW; (b) salt excess due to LIW.

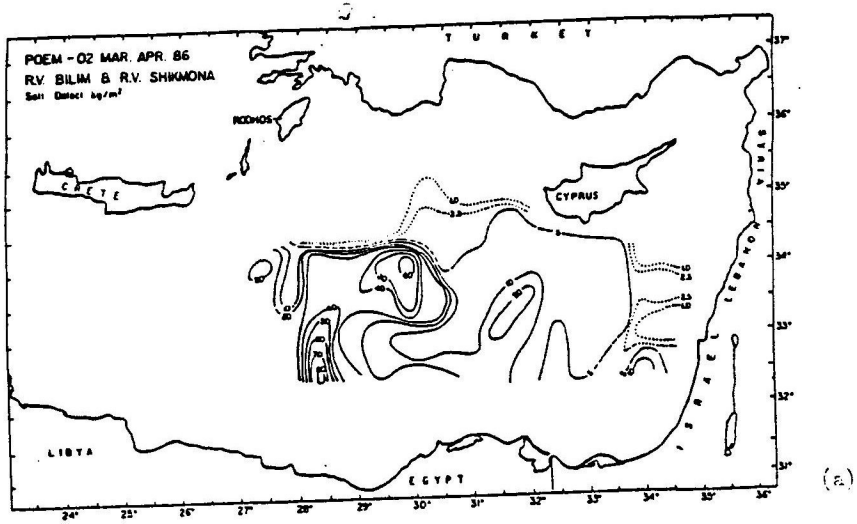

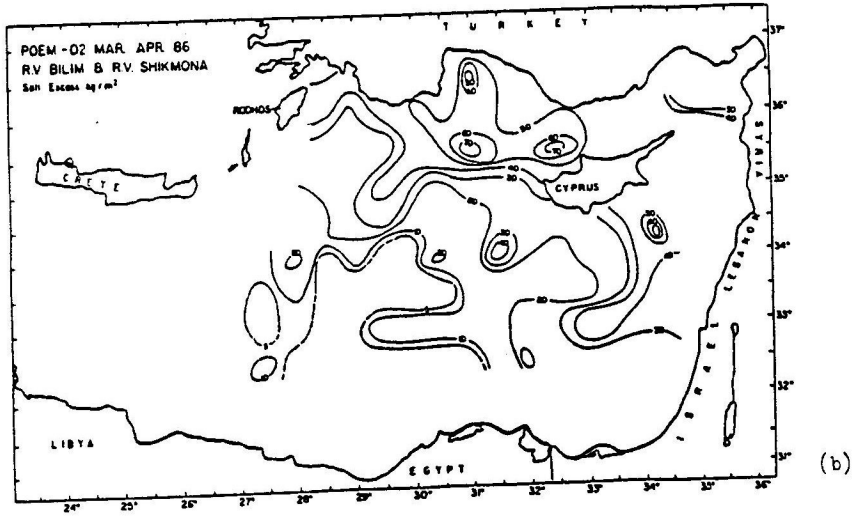

Fig. 7 Salt anomaly in units of kg m^{-2} integrated over the depth, March-April 1985. (a) Salt defect due to AW; (b) salt excess due to LIW.

Second POEM Scientific Workshop

OSSERVATORIO GEOFISICO SPERIMENTALE

Trieste, Italy

31 May – 4 June, 1988

POEM Scientific Reports #3

Cambridge, Massachusetts

August 1989